Well Detection in Satellite Images using Convolutional Neural Networks

Pratik Sanjay Wagh, Debanjan Das* and Om P. Damani

Department of Computer Science & Engineering, IIT Bombay, Mumbai, India

Keywords: Remote Sensing, Computer Vision, Object Detection, Convolutional Neural Networks, Machine Learning.

Abstract: The Government of India conducts a well census every five years. It is time-consuming, costly, and usually incomplete. By using transfer learning-based object detection algorithms, we have built a system for the automatic detection of wells in satellite images. We analyze the performance of three object detection algorithms - Convolutional Neural Network, HaarCascade, and Histogram of Oriented Gradients on the task of well detection and find that the Convolutional Neural Network based YOLOv2 performs best and forms the core of our system. Our current system has a precision value of **0.95** and a recall value of **0.91** on our dataset. The main contribution of our work is to create a novel open-source system for well detection in satellite images and create an associated dataset which will be put in the public domain. A related contribution is the development of a general purpose satellite image annotation system to annotate and validate objects in satellite images. While our focus is on well detection, the system is general purpose and can be used for detection of other objects as well.

1 INTRODUCTION

Automation of well records promises to be a big step in developing countries' E-governance initiatives. Currently, the well census in India is conducted every five years and in between, farmers are supposed to contact the nearest revenue department office to get their land records updated with their well information. This is rarely done, especially due to complex ownership issues. Many government schemes offered to farmers are contingent upon the assets held by the farmer, e.g. to qualify for the drip irrigation subsidy, and farmers are unable to take benefit of these schemes when records are not up-to-date.

Not just for individual farmers, but for the country as a whole, it is important to have good data on groundwater use for planning and governance (Ministry of Water Resource, 2006a). For example, the Central Groundwater Board estimates the country's net irrigated area and irrigation potential using the well count and the counts of other ground and surface water sources obtained through the minor irrigation census. The process of estimating a watershed's groundwater development also requires the estimate of groundwater use which uses the well count data.

There are several administrative and resource-related challenges (Ministry of Water Resource, 2006b) in conducting the well census. This surveying process is time-consuming, lengthy, and cost ineffective due to which the collected data is often incomplete and potentially corrupt. As a first step towards solving this problem, we exploit the recent advances (Redmon et al., 2015; LeCun et al., 1999; Viola and Jones, 2001; Dalal and Triggs, 2005; Albert et al., 2017) in the area of applied machine learning and computer vision, to automate the task of maintaining well records. Later, we can overlay the cadastral maps giving land ownership, with GIS maps with detected wells, and classify well ownership by class, caste, regions etc (Ministry of Water Resource, 2006c).

The task of automatic well detection is challenging since the actual real-life well looks quite different from the wells present in satellite images. The contrast is depicted in Figure 2. This implies that object detection methods that work well for real-life camera images may not be suitable for object detection in satellite images.

We observe that the wells in the Google Maps images are like dark circular shaped objects with a thin white cyclic patch around it. A further challenge in automatic well detection is that sizes of the wells in developing countries are such that they generally look very similar to tree or shadow of the trees (Figure 2), and parts of the well maybe covered by the trees. This poses challenge even for human annotators.

* This author is also co-first author.

Wagh, P., Das, D. and Damani, O.
Well Detection in Satellite Images using Convolutional Neural Networks.
DOI: 10.5220/0007734901170125
In *Proceedings of the 5th International Conference on Geographical Information Systems Theory, Applications and Management (GISTAM 2019)*, pages 117-125
ISBN: 978-989-758-371-1

Figure 1: Contrast between real-life well and wells in satellite images (Maitra, 2011).

Figure 2: Similarity between well and shadow of a tree in a satellite image.

While the analysis of satellite imagery is quite an old field, the application of deep learning in this area is a new and emerging trend. Existing work in the area focuses on detection of man-made objects in satellite images, e.g, air-crafts(Wu et al., 2015), vehicles(Chen et al., 2014) and oil tanks(Zhang et al., 2015). All of these works follow a process pipeline approach. First, the object is localized, then it is recognized, and then the classification happens. The binarized normed gradients (Cheng et al., 2014) is used in (Wu et al., 2015) to localize the air-crafts present in a satellite image and then a Hybrid Deep Convolutional Neural Network is used for feature extraction, and for classification support-vector machines (Vapnik, 1999) is used. Similarly, in (Zhang et al., 2015), the object of interest is oil-tanks, and hence the elliptical or circular shapes in an image are detected using ellipse and line segment detector. After object localization, they use Histogram of Oriented Gradients (Dalal and Triggs, 2005) and Convolutional Neural Networks methods for feature extraction.

All of these methods require large training sets. In the area of urban planning where training data is scarce, the concept of transfer learning is used in (Albert et al., 2017) for object classification and feature extraction.

In the context of general object detection algorithms, we first worked with the basic Convolutional Neural Network architectures (LeCun et al., 1999), HaarCascade (Viola and Jones, 2001) and Histogram of Oriented Gradients (Dalal and Triggs, 2005) with support-vector machine (Vapnik, 1999) methods. However, we achieved limited success towards well detection with these approaches.

Then, inspired by the success of transfer learning approach in urban planning context (Albert et al., 2017), we decided to experiment with the transfer learning technique in the context of rural planning. We experimented with the popular single shot object detection algorithms *You Only Look Once* (YOLOv2 (Redmon and Farhadi, 2016)). In this work, the problem of object detection is framed as a regression problem where it outputs the probable bounding box coordinates and the class probabilities for each bounding box. YOLO uses Deep Convolutional Neural Networks for image recognition and bounding box drawing. In contrast to the pipeline approaches, it performs the object detection in the single shot, which makes it a lot faster than other object detection algorithms.

In the literature, several authors lament the scarcity of good quality data for object detection in satellite images and manually collect data from different sources. For our well detection problem also, there is no existing satellite image dataset with wells identified in it. As we collaborated with members of the Rural Development Department for data collection, we realized the need for a proper system to annotate and validate wells in the satellite images. To our surprise, no such system was available in the public domain. Hence, we decided to develop a general purpose satellite image annotation system (SIAS) using which one can annotate and validate objects of any type in satellite images.

The contribution of our work is two-fold. The main contribution of our work is to create a novel open-source transfer learning based system for well detection in satellite images and create an associated dataset to be put in the public domain. A related contribution is the development of a general purpose satellite image annotation system to annotate and validate objects in satellite images. While our focus is on well detection, the system is general purpose and can be used for detection of other objects as well.

In Section 2, we discuss our SIAS system. Section 3 describes the object detection algorithms which we have used, in Section 4 we discuss about the dataset, performance metric we used and the training procedure we followed and the last section contains the conclusions.

2 SYSTEM ARCHITECTURE

In addition to experimenting with machine learning algorithms, it is important to build a system that is intuitive to use for end users. In our case, end users will be government officials who may not be very computer savvy. Hence we developed a web-based application that can be used across the internet. Further, the same system should be capable of taking feedback from the user where the user can validate or invalidate the detected well. A user should also be able to mark an undetected well. In fact, this feedback should flow into the system and get added to the training set. This way the training set will keep growing over time as the system gets used. We call our system SIAS - Satellite Image Annotation System.

The architecture diagram of the whole system is given in Figure 3.

2.1 User Interface

We follow the Software As A Service (SaaS) model. At the backend, we use Flask (Ronacher, 2010) which is a micro-web framework. The frontend is developed with HTML, CSS, and JavaScript. The user interface is shown in Figure 4.

2.1.1 Frontend

The adoption of the system critically depends on the user-friendliness of the frontend. Various features of frontend are listed below.

- It contains a search bar and a map window where one can search for a place and the resulting satellite image is shown in that window.
- There is an optional field, using which we can select the model we want to use. The available models are YOLOv2, tinyYOLOv3, Basic Convolutional Neural Network model, the Histogram of Oriented Gradients-support-vector machines and HaarCascade.
- After searching for a place and selecting the model, clicking on ”Predict” button shows the predicted wells in that area with the help of bounding boxes. These bounding boxes are superimposed on the satellite image.
- Note that user can select an arbitrarily large area to predict. We subdivide the selected area into multiple blocks of size 640×640. Each of these blocks is then given as input to the selected model. Currently, if a well falls on the boundary of two sub-blocks then it is not detected. In the future, we plan to solve this problem by creating different partition sets of the same area and merging the results from these partition sets.
- An important feature of the system is that it provides the user ability to give feedback. Each of the predicted boxes can be marked as valid or invalid by the user. This way the training set will keep growing over time as the system gets used.
- The user can also label any object of interest in the image by selecting and marking the corresponding area.

2.1.2 Backend

The backend acts as a bridge between the object detection models and frontend. Images from frontend come in the form of a base64 string. In the backend, it is decoded and converted into PNG images and the model is applied to it. The output image is then sent back to the frontend.

3 OBJECT DETECTION ALGORITHMS

We experimented with various object detection methods and found that transfer learning based YOLO model performs the best. We next describe the methods tried.

3.1 Basic Convolutional Neural Network

In this model we have used CNN as a feature extractor and multi-layer perceptron (MLP) as a classifier. We have created a two-layered Convolutional Neural Network (CNN) model. The description of the model is given as:

- The first convolutional stage is with rectified linear unit (ReLU) activation function followed by a max-pooling layer. This layer has 20 convolutional filters, each one of them has a size of 5×5. The output dimension is the same as that of the input shape i.e, 64×64. As this is the first layer in our model, we have to define its input shape i.e, (1,64,64). The max-pooling operation applies a sliding window that slides over the image and

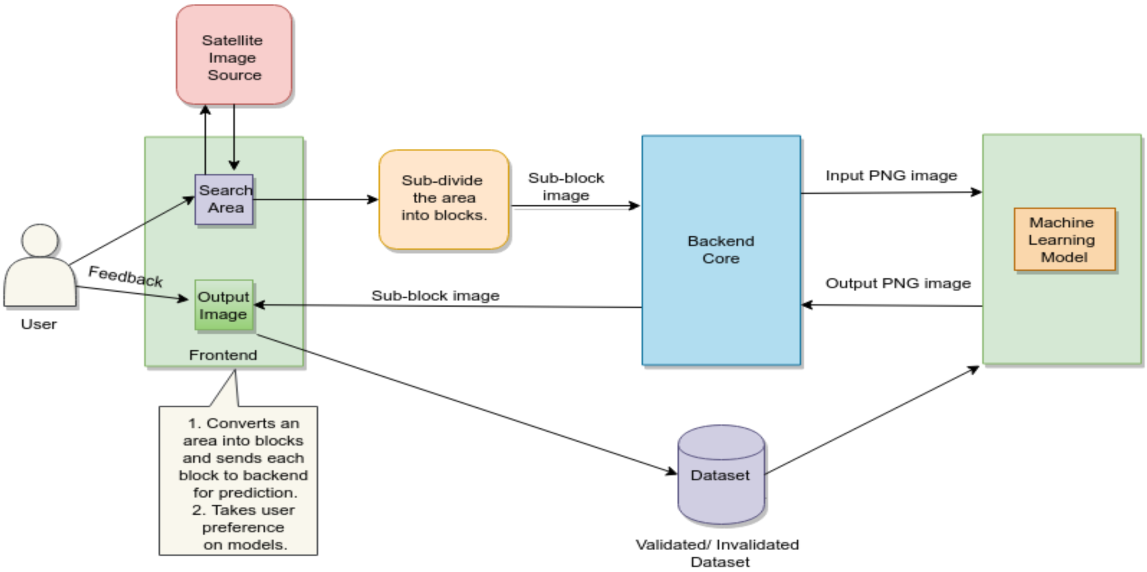

Figure 3: SIAS system architecture.

Figure 4: User interface of the SIAS system.

takes the maximum value of the pixel present in that region.

- The second convolutional layer is also followed by rectified linear unit activation function and a max-pooling layer. Now, we increase the number of convolutional filters to 50 from 20 in the previous layer.
- Then we have a standard flattening layer and a dense layer of 500 neurons. This flattening layer flattens the last 3D feature block of the CNN and provides it to the dense layer. This dense layer acts as a hidden layer. The output layer of the MLP has softmax function as activation function, which can be defined as:

$$P(y=j|X) = \frac{e^{X^T \cdot w}}{\sum_{k=1}^{K} e^{X^T \cdot w}}$$

where K is the number of classes and $P(y = j|X)$ is the probability of the input being in class j given it's feature vector X.

3.2 HaarCascade

Introduced in 2006, it has been very successful at face detection problem(Viola and Jones, 2001). Since then it has been used for various other object detection problems which use non-satellite images. It uses the Haar-like feature for detecting an object. It has introduced an integral image for efficient and quick calculation of the sum of pixel values in a rectangular subset of the given image, thus lowers the computation time. It uses AdaBoost classifier for classifying the positive and negative feature.

3.3 HOG

Histogram of Oriented Gradient (HOG)(Dalal and Triggs, 2005) is a feature descriptor method. This method uses the orientation of an image as a feature for detecting an object thus generalizes well for the objects which have a fixed shape. It first divides the image into small connected blocks which consist of cells and then computes the histogram of the gradient for each pixel within the cell. Then it discretizes each cell into angular bins according to the gradient orientation. Each cell is combined to form blocks, these blocks are normalized and used as a feature descriptor which is used with support-vector machine (Vapnik, 1999) for object detection.

3.4 YOLOv2

You Only Look Once (YOLOv2) (Redmon and Farhadi, 2016) introduced in late 2016 gave a mean Average Precision (mAP) of 76.8 on VOC 2007 dataset, is an improved version of the YOLOv1 (Redmon et al., 2015). Unlike the traditional network, it uses a single neural network for object classification and detection. It divides the whole image into grids of small boxes and each box is responsible for detecting and predicting the class. The whole process occurs in one pass thus a global context of an image is available for detecting the object in an image. It uses batch normalization, high-resolution classifier, convolution with anchor boxes, direct location prediction, and multiscale prediction.

It uses Darknet-19 as base model which consists of 19 convolutional layers and 5 max-pooling layers which requires 5.58 billion operations to process an image thus making it faster.

3.5 YOLOv3

YOLOv3 (Redmon and Farhadi, 2018) is the successor approach for the YOLOv2. It was introduced in 2018 and incorporated some of the drawbacks present in YOLOv2 such as upsampling, skip connections and residual blocks. It works in a similar way as the YOLOv2 with some variation in the architecture. It uses Darknet-53 as the base model which consists of 106 convolutional layers making it slow in detection. The accuracy is increased due to the use of 1x1 detection kernel at three different scale. It uses 9 anchor boxes instead of 5, 3 at each different scale. This anchor box is arranged in the descending order of dimensions and thus detects the 10x more no. boxes than YOLOv2.

4 EXPERIMENTAL RESULTS

As mentioned before, different object detection methods require different dataset for training and follow different training and testing procedure. We next describe below the dataset which we used for each object detection method, performance measure, and the training procedure which we followed.

4.1 Dataset Description

The uniqueness of the problem resulted in data scarcity. Well detection is a completely new problem that does not have any dataset as per the best of our knowledge. The dataset we used for each object detection algorithm is described below :-

- *Basic Convolutional Neural Network*: We have prepared a different dataset of ground truth images of well and non-well images. We have manually collected the coordinates of the wells and downloaded the image of that coordinate from Google Earth at zoom level of 19. We have collected around 769 well images and 700 non-well images of size 64×64.

  For training the model, 500 well images and 500 non-well images are used. And for testing the model 269 well images and 200 non-well images have been used.

- *HaarCascade*: We trained Haarcascade for a different dataset as it requires two sets of data i.e positive data which only contains the well image and the negative data which do not contain the well image. Thus we have manually collected the coordinates of the wells and non-wells (which is anything except well) and downloaded the image of that coordinate from Google Earth at a zoom level of 19. We trained using 1721 positive images which has a dimension of 64 x 64 and 3035 negative images which has a dimension of 114 x 114.

- *YOLOv2 and tinyYOLOv3*: We developed a dataset of 1068 images of resolution 640×640 from Google Maps Static API at a zoom level of 19. Each image contains multiple wells. We had drawn ground truth bounding boxes around the wells in an image using BBox-Label-Tool (Qiu, 2017).

  We collected the images from 20 different districts of Maharashtra state. Out of which training data consists of 535 images from 10 districts and testing data consists of 403 images from other 10 districts. We randomly extracted 130 images from the districts of Maharashtra state as a validation dataset. We trained the model for 535 images and validated it on a set of 130 images. After validation we found that out of 130 images, 100 images were such in which most of the wells present were not getting detected, so we added those 100 images to the training dataset, thus totalling the training dataset to 635 images and then retrained our model for this set.
- *HOG*: Thus to compare HOG with YOLO models we extracted the wells present in the images of training dataset, which we described in the YOLO model section consisting of 635 images, at a dimension of 150 x 150 which totals to 1022 positive images. Then we annotated the images using imglab tool and trained HOG on the newly created dataset along with the annotated file.

4.2 Performance Measure

To evaluate the performance of our model we used some metrics which helped us to find the best object detection algorithm for our model. Description related to our context along with the formula is listed below.

- Precision: It is the fraction of the wells detected among all the detections in an image. The formula for calculating the precision is given below.

$$Precision = \frac{True\ Positives}{True\ Positives + False\ Positives}$$

- Recall: It is the fraction of the wells detected among all the wells present in an image. The formula for calculating the recall is given below.

$$Recall = \frac{True\ Positives}{True\ Positives + False\ Negatives}$$

- F1 Score: It is the harmonic mean of Precision and Recall and the formula for the F1 score is given below.

$$F1score = 2 \times \frac{Precision \times Recall}{Precision + Recall}$$

4.3 Training

Different methods follows different training procedure thus we mentioned one by one training procedure which we followed for each method :-

- *Basic Convolutional Neural Network* The results of deploying the above mentioned trained model on 469 test images are given below:
  - **Test accuracy Score**: 0.92
  - **Correctly classified images**: 435
  - **True Negatives**: 211
  - **True Positives**: 224
  - **False Positives**: 19
  - **False Negatives**: 15
  - **Precision**: 0.92
  - **Recall**: 0.93

  Although the results of the model looks promising on this dataset but it performed poorly on the other dataset, i.e, dataset from a different geographical region. This model takes images of 64×64 resolution and predicts whether it is well or not. Thus deploying this model on 640×640 images required proper object localization procedures. Upon applying sliding window approach, we found out that the number of false positive were very high i,e, the precision was very low but the true positive rate or the recall was high. Thus we dropped this method from comparison. Some results are shown in figure 5.

Figure 5: Results of Basic CNN on 640×640 images.

- *HaarCascade* We trained using 1721 positive images and 3035 negative images and the results obtained are shown in Figure 6. As can be seen in Figure 6 the results obtained were terrible and improving them will require a much larger number of positive and negative images which was not feasible for us. Thus we dropped this algorithm from comparison.

(a) (b)

Figure 6: (a) and (b) are results obtained from Haarcascade method.

- *HOG*

  We trained HOG using dlib on a machine which has 8 GB RAM. The training was configured with a learning rate of 0.01, epsilon value of 5 and sliding window of 83 x 77 pixel.

  The results obtained can be seen in Figure 7 which are promising thus we used this method for comparison with other models.

(a) (b)

Figure 7: (a) and (b) are results obtained from HOG method.

- *YOLOv2*

  For training YOLOv2 and using it for detection we used darknet framework. The training was performed on the standard configuration of YOLOv2-VOC (yolov2-voc.cfg) it has a learning rate of 0.001, the batch size of 64 and subdivisions of 8. We used a weights file already pretrained on Imagnet dataset (Russakovsky et al., 2015) and trained on GPU (Nvidia Titan XP) for 20000 iterations. The object detection was performed on the default threshold value of 0.25 or more.

  The results obtained are shown in Figure 8. This result obtained is the best result achieved as compared to methods which we discussed till now.

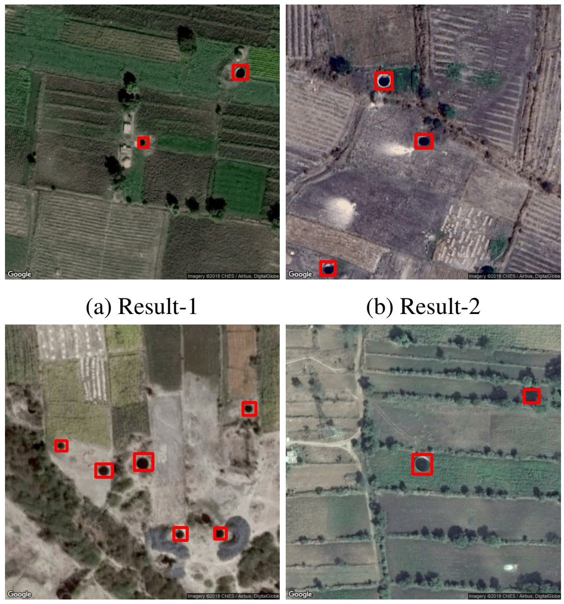

(a) Result-1 (b) Result-2

(c) Result-3 (d) Result-4

Figure 8: Results from YOLOv2 obtained from the weight file trained for 20000 iterations.

- *tinyYOLOv3*

  We used the Darknet framework for training and detection. The training was performed on the standard configuration of yolov3-tiny which is a constrained network of YOLOv3 (yolov3-tiny-obj.cfg) it has a learning rate of 0.001, the batch size of 64 and subdivisions of 8 We used a weights file already pretrained on Imagnet dataset (Russakovsky et al., 2015) and trained on GPU (Nvidia Titan XP) for 20000 iterations. The object detection was performed on the default threshold value of 0.25 or more. Similar results as YOLOv2 were obtained for the images in Figure 8.

4.4 Retraining Surprise

One would think that inclusion of an image set in training set will ensure that the trained model will give high detection accuracy on that image set. However, while this holds true for YOLO, surprising this is not true for other object detection algorithms that we experimented with.

We validated the weights file obtained from training for 130 well images extracted randomly from any district present in Maharashtra state for YOLO models. After validation, we found that in 100 images from the validation dataset some of the wells present were not getting detected thus we added those 100 images to the training dataset and retrained the network for 20000 iterations. The results obtained before and after retraining can be seen in Figure 9.

(a) (b) (c) (d)

Figure 9: Figure (a), (c) are results obtained from YOLOv2 before validation and Figure (b), (d) are corresponding results after validation and retraining on YOLOv2.

The results show that if we retrain YOLO model by including images in which wells were not getting detected then the retrained model is able to detect the similar wells which were not getting detected earlier. This might be because the wells which were not getting detected vary totally from the images for which we have trained our model.

For the other object detection methods not based on transfer learning, even after retraining the model by including such images in training dataset, similar wells present in other images were not getting detected. We have not been able to ascertain the reason for the same.

4.5 Results

For testing we extracted 403 well images from 9 districts of Maharashtra which includes Solapur, Kolhapur, Hingoli, Ratnagiri, Beed, Aurangabad, Chandrapur, Jalna, and Satara.

Then we tested the weights file of YOLOv2 and tiny YOLOv3 obtained from 20000 iterations and HOG using the svm file obtained after training on the testing dataset.

The results can be seen in Table 1.

Thus the obtained precision and recall value on the testing dataset for YOLOv2 is **0.95** and **0.91**, for tiny YOLOv3 is **0.98** and **0.84** and for HOG is **0.95** and **0.34** respectively.

Table 1: Performance comparison of YOLOv2, tiny YOLOv3 and HOG model.

Metric	Model		
	YOLOv2	*tiny YOLOv3*	*HOG*
True Positive	592	529	226
False Positive	29	9	12
False Negative	58	100	430

Table 2: Precision-Recall trade-off between YOLOv2, tiny YOLOv3 and HOG.

Model	Precision	Recall	F1 Score
YOLOv2	0.95	0.91	0.92
tiny YOLOv3	0.98	0.84	0.90
HOG	0.95	0.34	0.51

The precision-recall trade-off between these algorithms is shown in Table 2. Based on these results, our system uses YOLOv2 by default, but we provided the option to user to chose tiny YOLOv3, HOG or other algorithms if they wish.

5 CONCLUSIONS

We have built an open source system for well detection in satellite images and an associated annotation system to annotate and validate identified objects in satellite images. The advantage of the annotation system is that we can use it to continuously grow our dataset. We plan to use data augmentation technique to create a larger dataset for transfer learning. Also, YOLO was pre-trained on ImageNet (Russakovsky et al., 2015) dataset which is very different from satellite images. For the future work, we want to train YOLO on some satellite image dataset, e.g, xView dataset (Experimental, 2018). On top of that, we can train it on our enhanced well dataset. Also, further experimentation with several single shot object detection algorithms has to be done along with transfer learning to develop a robust system. Our aim would be to generalize this satellite image object detection procedure as much as possible to several classes of objects.

REFERENCES

Albert, A., Kaur, J., and Gonzalez, M. C. (2017). Using convolutional networks and satellite imagery to identify patterns in urban environments at a large scale. *CoRR*, abs/1704.02965.

Chen, X., Xiang, S., Liu, C., and Pan, C. (2014). Vehicle detection in satellite images by hybrid deep convolutional neural networks. *IEEE Geoscience and Remote Sensing Letters*, 11(10):1797–1801.

Cheng, M., Zhang, Z., Lin, W., and Torr, P. (2014). Bing: Binarized normed gradients for objectness estimation at 300fps. In *2014 IEEE Conference on Computer Vision and Pattern Recognition*, pages 3286–3293.

Dalal, N. and Triggs, B. (2005). Histograms of oriented gradients for human detection. In *2005 IEEE Computer Society Conference on Computer Vision and Pattern Recognition (CVPR'05)*, volume 1, pages 886–893 vol. 1.

Experimental, D. I. U. (2018). Diux xview 2018 detection challenge (http://xviewdataset.org).

LeCun, Y., Haffner, P., Bottou, L., and Bengio, Y. (1999). Object recognition with gradient-based learning. In *Shape, Contour and Grouping in Computer Vision*, pages 319–, London, UK, UK. Springer-Verlag.

Maitra, M. K. (2011). Frequently asked questions (faq) on groundwater - understanding the basics (http://www.indiawaterportal.org/articles/frequently-asked-questions-faq-groundwater-understanding-basics).

Ministry of Water Resource, G. o. I. (2006a). Census of minor irrigation schemes (http://micensus.gov.in/censusmisch.html).

Ministry of Water Resource, G. o. I. (2006b). Methodology of minor irrigation census (http://micensus.gov.in/methodology.html).

Ministry of Water Resource, G. o. I. (2006c). National level report - dugwell (http://micensus.gov.in/dugnat.html).

Qiu, S. (2017). Bbox-label-tool (https://github.com/puzzledqs/bbox-label-tool).

Redmon, J., Divvala, S. K., Girshick, R. B., and Farhadi, A. (2015). You only look once: Unified, real-time object detection. *CoRR*, abs/1506.02640.

Redmon, J. and Farhadi, A. (2016). YOLO9000: better, faster, stronger. *CoRR*, abs/1612.08242.

Redmon, J. and Farhadi, A. (2018). Yolov3: An incremental improvement. *CoRR*, abs/1804.02767.

Ronacher, A. (2010). Flask (http://flask.pocoo.org/).

Russakovsky, O., Deng, J., Su, H., Krause, J., Satheesh, S., Ma, S., Huang, Z., Karpathy, A., Khosla, A., Bernstein, M., Berg, A. C., and Fei-Fei, L. (2015). Imagenet large scale visual recognition challenge. *Int. J. Comput. Vision*, 115(3):211–252.

Vapnik, V. N. (1999). An overview of statistical learning theory. *IEEE Transactions on Neural Networks*, 10(5):988–999.

Viola, P. and Jones, M. (2001). Rapid object detection using a boosted cascade of simple features. In *Proceedings of the 2001 IEEE Computer Society Conference on Computer Vision and Pattern Recognition. CVPR 2001*, volume 1, pages I–I.

Wu, H., Zhang, H., Zhang, J., and Xu, F. (2015). Fast aircraft detection in satellite images based on convolutional neural networks. In *2015 IEEE International Conference on Image Processing (ICIP)*, pages 4210–4214.

Zhang, L., Shi, Z., and Wu, J. (2015). A hierarchical oil tank detector with deep surrounding features for high-resolution optical satellite imagery. *IEEE Journal of Selected Topics in Applied Earth Observations and Remote Sensing*, 8(10):4895–4909.